

Ultimate Performance of a Cold-Electron Bolometer with Strong Electrothermal Feedback

Leonid Kuzmin

Chalmers University of Technology, Department of Microtechnology and Nanoscience 41296 Gothenburg, Sweden

ABSTRACT

A novel concept of the Cold-Electron Bolometer (CEB) with strong electrothermal feedback has been proposed. The concept is based on *direct electron cooling* of the absorber that serves as negative electrothermal feedback for incoming signal. This feedback is analogous to TES (transition-edge sensor) but additional dc heating is replaced by deep electron cooling to minimum temperature. It could mean a principle breakthrough in realization of supersensitive detectors. Noise properties are considerably improved by decreasing the electron temperature. The loop gain of electrothermal feedback could exceed 1000. The response time is reduced by electrothermal feedback to 10ns in comparison with the intrinsic e-ph time constant of 10 μ s.

The CEB gives opportunity to increase dynamic range by removing all incoming power from supersensitive absorber to the next stage of readout system (SQUID) with higher dynamic range. Saturation problems are not so severe for CEB as for TES: after exceeding the cooling power there is only slight deviation from linear dependence for voltage response. The full saturation comes at the level of 100pW when temperature of absorber achieves T_c of Al. Ultimate performance of the CEB is determined by shot noise of the signal readout. For background load $P_0 = 10$ fW and quantization level $T_e = 50$ mK, the limit NEP is equal to 10^{-19} W/Hz $^{1/2}$. The estimations show that it is realistic to achieve ultimate NEP at 100 mK with SQUID readout system and NEP= 10^{-18} W/Hz $^{1/2}$ at 300mK for background load of 10fW. Applicability of the CEB to post-Herschel missions looks very promising.

INTRODUCTION

As it has been recognized by Science [1], the Breakthrough of the Year has been “*Illuminating the Dark Universe*”. The portraits of the earliest universe made in microwaves by the Wilkinson Microwave Anisotropy Probe confirm that the Universe is made up largely of mysterious *dark energy and dark matter*. To understand the nature of them,

the future cosmology needs to get a more detailed picture of the **cosmic microwave background**. The proposed NASA missions SPIRIT, SPECS, and SAFIR will determine the highest level of requirements for bolometers in nearest future.

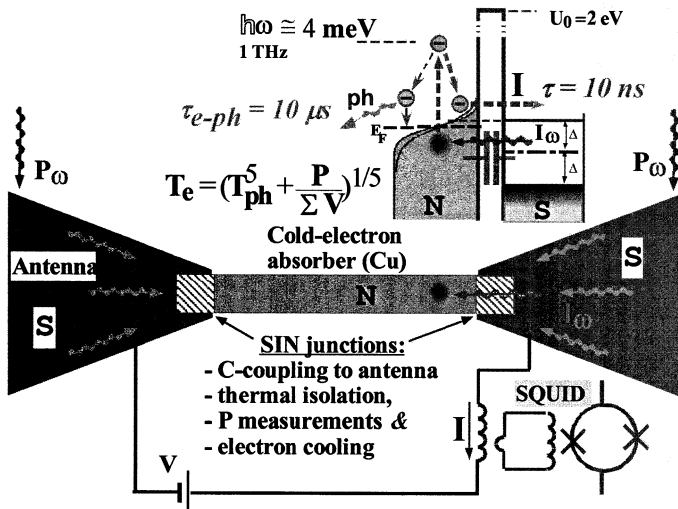


Fig. 1. Capacitively coupled Cold-Electron Bolometer with SIN tunnel junctions for direct electron cooling and power measurements. The signal power is supplied to sensor through capacitance of tunnel junctions, dissipated in cold-electron absorber, and removed back from the absorber as hot electrons by the same SIN junctions. The electron cooling serves as strong negative electrothermal feedback improving all characteristics of the CEB (time constant, responsivity) and NEP.

The detector goal is to provide noise equivalent power down to 10^{-20} W/Hz $^{1/2}$ [2] over the 40 – 500 μ m wavelength range in a 100x100 pixel detector array with low power dissipation array readout electronics. *No one existing technology could satisfy these requirements.* Technological breakthrough should be done, first of all, to approach these requirements. The analysis shows that the proposed concept of ultimate CEB with strong electrothermal feedback has a real chance to become a leading concept in this development.

Decisive step in development of superconducting detectors has been innovation of a TES with strong electrothermal feedback [3,4]. However, the TES has some problems with excess noise, saturation, and the most

with artificial overheating by dc power for the feedback. This additional heating kills all efforts on deep cooling and does not give good perspectives for realization of limit performance of the bolometer. In contrast to this overheating, the principle new concept of a “Cold-Electron” Bolometer (CEB) with direct electron cooling has been proposed by Kuzmin et al. [5-8]. The CEB is the only concept suggesting removing incoming background power from supersensitive region of absorber. The CEB avoids the main problem of TES, an *additional dc heating* for the electrothermal feedback, and replace it with *the direct electron cooling* of the absorber that could be a *turning point* in realization of modern supersensitive detectors. This cooling could be especially important for the realization of high sensitivity in presence of the realistic background power load. It could help to avoid full saturation when signal exceeds the level of dc bias power that is the great problem for the TES. The CEB could give a high dynamic range in combination with SQUID readout system having high dynamic range in closed-loop operation. All power of the signal is used for measurements. Possible objection that tunneling of electrons would increase shot noise is rejected by simple argument: if power is not removed by tunnel junctions, the same type of shot noise will be created by phonons through increased electron-phonon interaction.

Comparison of CEB and TES

The operation of CEB can be analyzed using heat balance equation [7,8]:

$$P_c(V, T_e, T_{ph}) + \Sigma \Lambda (T_e^5 - T_{ph}^5) + C_\Lambda \frac{dT}{dt} = P_0 + \delta P(t) \quad (1)$$

Here, $\Sigma \Lambda (T_e^5 - T_{ph}^5)$ is the heat flow from electron to the phonon subsystems in the normal metal, Σ is a material constant, Λ - a volume of the absorber, T_e and T_{ph} are, respectively, the electron and phonon temperatures of the absorber; $P_{cool}(V, T_e, T_{ph})$ is cooling power of the SIN tunnel junctions; $C_v = \gamma T_e$ is the specific heat capacity of the normal metal; and $P(t)$ is the incoming rf power. We can separate Eq. (1) into the time independent term,

$\Sigma \Lambda (T_{e0}^5 - T_{ph0}^5) + P_{cool0}(V, T_{e0}, T_{ph0}) = P_0$, and time dependent: $(\partial P_{cool} / \partial T + 5 \Sigma \Lambda T_e^4 + i \omega C_\Lambda) \delta T = \delta P$. The first term, $G_{cool} = \partial P_{cool} / \partial T$, is the cooling thermal conductance of the SIN junction that gives the negative electrothermal feedback (ETF); when it is large, it reduces the temperature response δT because cooling power, P_{cool} , compensates the change of signal power in the bolometer. The second, $G_{e-ph} = 5 \Sigma \Lambda T_e^4$, is electron-phonon thermal conductance of the absorber. From Eq. (2) we define an effective complex thermal conductance which controls the temperature response of CEB to the incident signal power

$$G_{eff} = G_{cool} + G_{e-ph} + i \omega C_\Lambda \quad (2)$$

In analogy with TES [3,4], the effective thermal conductance of the CEB is increased by the effect of electron cooling (negative ETF). The current responsivity is given by

$$S_i = \frac{\partial I}{\partial P} = \frac{\partial I / \partial T}{G_{cool} + G_{e-ph} + i \omega C_\Lambda} = \frac{\partial I / \partial T}{G_{cool}} \frac{L}{(L+1) [1 + i \omega \tau]} \quad (3)$$

where

$$L = G_{cool} / G_{e-ph} \gg 1 \quad \text{is ETF gain and} \quad \tau = C_\Lambda / G_{e-ph} = \tau_0 / (L+1) \quad (4)$$

is an effective time constant, $\tau_0 = C_\Lambda / G_{e-ph}$ ($\cong 10 \mu s$ at 100 mK).

The principle of operation of CEB and TES in voltage-biased mode is shown in Fig. 2 and 3. The TES is heated to T_c by dc power P_{bias} . This temperature is supported during all range of operation (before saturation) due to electrothermal feedback. The principle of operation of the CEB is approximately the same but moving to another bias point in temperature: to absolute zero. Starting from the phonon temperature $T_{ph}=100$ mK, the cooling conductance, G_{cool} , decrease the electron temperature to the possible minimum level. Dependence of output power on signal power is shown in Fig. 3. For both concepts P_{out} is nearly equal to incoming power in the range of dc heating power (TES) and typical cooling power (CEB). Accuracy of removing (CEB) or compensation (TES) of incoming power is determined by the strength of the electrothermal feedback - loop gain L .

For TES, the L is determined by nonlinearity of $R(T)$ dependence and could exceed 1000. For CEB, the L is determined as relation of thermal conductances (5). Typical dependence of L on incoming power is shown in Fig. 4. The saturation problem is very serious for TES: P_{sat} is exactly equal to applied dc heating power P_{bias} (Fig. 3). After

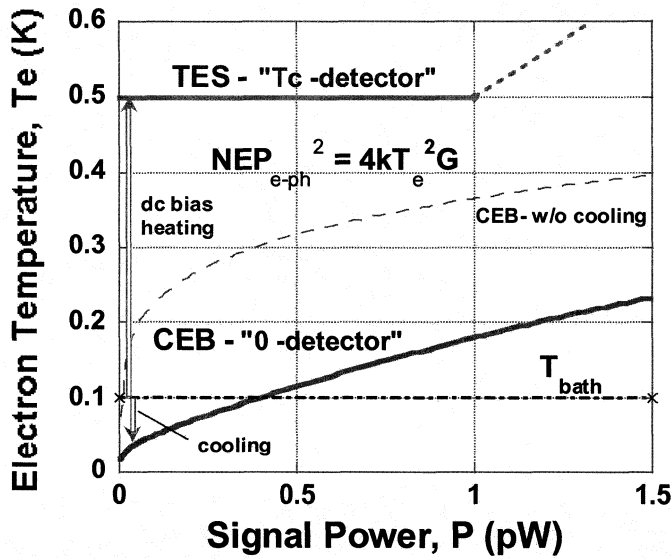
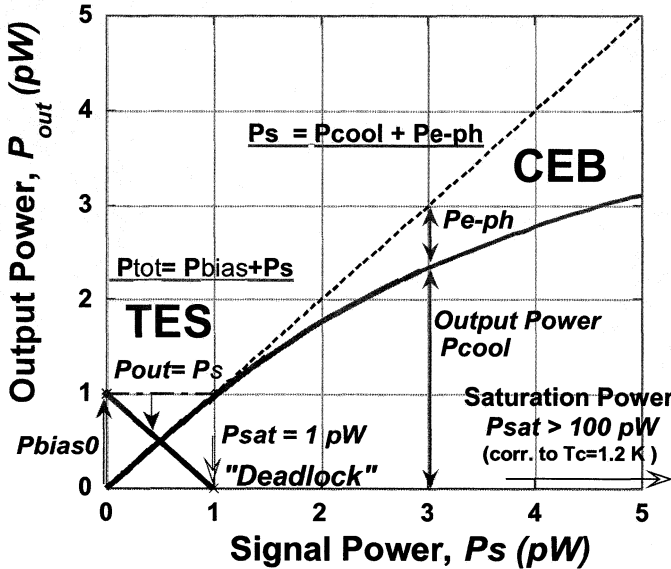


Fig. 2. Electron temperature as a function of signal power for $T_{bath}=100$ mK for CEB and TES. For CEB, the T_e is always cooled to possible minimum level. For $P < 0.4$ pW, the T_e of CEB is less than T_{bath} (real Cold-Electron Bolometer). For TES, the T_e is equal to T_C for all range of operation up to saturation power. After saturation there is uncontrollable increase of temperature.



saturation power, the TES fully stops operation. It is difficult to foresee the expected level of maximum power load and choose of P_{sat} is really complicated problem. Absolutely different situation is for CEB saturation: the output cooling power would simply deviate from the linear dependence $P_{cool}(P)$. For the typical cooling power around 1 pW, the deviation from linear

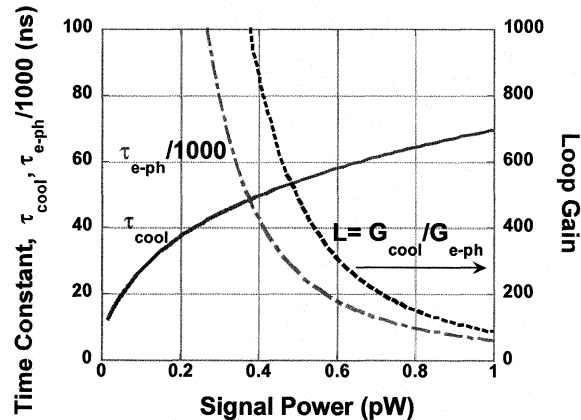
Fig. 3: Output power of CEB (P_{cool}) and TES ($-\delta P_{bias}$) in dependence on Signal power. They are almost equal at small level of power. At higher level of power, the signal power P is split between P_{cool} and P_{e-ph} . The Saturation power would be achieved only after heating to T_c of Al electrode (P_{sat} is around 100 pW). Output power of TES is equal to reduce in bias power proportional to signal power. Saturation power is equal to zero bias power with full "deadlock" after this value.

dependence $P_{out}(P)$ would be only several % at this level (Fig. 3). As signal power is further increased, the deviation will be larger but CEB still continue to work. It is the question of only calibration of this dependence. Final "deadlock" for CEB would be at the level of power around 100

pW when temperature achieves the critical temperature of the Al electrode.

Time constant

Fig. 4. Time constant of CEB, τ_{cool} , in dependence on signal power P_s . The electron-phonon time constant, τ_{e-ph} , is shown for comparison (scaled 1000 times). The τ_{cool} is considerably shorter than τ_{e-ph} and difference is increased when we move to smaller signal power with stronger electron cooling. The loop gain L of negative electrothermal feedback is shown by dashed line. The loop gain is strongly increased for smaller P_s due to decrease of G_{e-ph} .



Time response of the CEB (4) in dependence on incoming power is shown in Fig. 4. As for TES, it is strongly reduced by loop gain L of electrothermal feedback (5). Cooling conductance G_{cool} is not dependent strongly on incoming power and slightly increased for smaller power (τ_{cool} is reduced). In contrast, the e-ph conductance, G_{e-ph} , is very dependent on power due to 4th power dependence on T_e and strongly reduced for low power (related τ_{e-ph} is increased). As final result, the L is considerably increased for smaller power and exceeds the level of 1000. It is interesting to remark that the time constant of CEB in current-biased mode will be increased in comparison with intrinsic e-ph time constant [7]. The reason is in decrease of the total thermal conductance of a bolometer due to negative voltage response of the junction (positive electrothermal feedback).

Ultimate Noise Performance of the CEB. General Limit Noise Formula

Noise properties are characterized by the noise equivalent power (NEP), which is the sum of three different contributions, and is defined as follows [7-9]:

$$NEP_{total}^2 = NEP_{e-ph}^2 + NEP_{SIN}^2 + \frac{\delta I^2}{S_I^2}, \quad NEP_{e-ph}^2 = 10k_B \Sigma \Lambda (T_e^6 + T_{ph}^6) \quad (6)$$

Here NEP_{NIS}^2 is the noise of the NIS tunnel junctions, and the term $\delta I^2/S_I^2$ is due to the finite sensitivity of the amplifier (SQUID) δI . The noise of the NIS junctions has three components: shot noise $2eI/S^2_I$, the fluctuations of the heat flow through the tunnel junctions and the correlation between these two processes [7-9]:

$$NEP_{SIN}^2 = \frac{\delta I^2}{S_I^2} - 2 \frac{\langle \delta P_{\omega} \delta I_{\omega} \rangle}{S_I} + \delta P_{\omega}^2 \quad (7)$$

Due to this correlation the short noise is decreased at 30-70%. Similar correlation in TES decreases Johnson noise.

The question about ultimate noise performance has arisen in relation to highest requirements on NEP for future NASA missions [2]. The question is how realistic are these requirements on $NEP=10^{-20}$ W/ Hz^{1/2}. Ultimate performance of CEB and other bolometers has been analyzed. Photon noise is not included in this analysis and should be added later as additional external noise. The NEP is determined by the shot noise due to the power load. The shot noise is treated in general sense including e-ph shot noise due to emission of phonons. Other sources of noise are neglected due to small values. For the level of $P_0 = 10$ fW, this limit can be achieved using low temperatures (~ 100 mK) and small volume of the absorber ($\Lambda \leq 0.003 \mu m^3$) when we can neglect the electron-phonon noise component.

General ultimate NEP formula for shot noise limitation has been derived:

$$NEP_{shot} = (2P_0 E_{quant})^{1/2} \quad (8)$$

where E_{quant} is an energy level of P_0 quantization:

$E_{quant} = k_B T_e$ –for normal metal absorber, $E_{quant} = \Delta$ –for superconducting absorber.

Ultimate NEP can be estimated for different bolometers for relatively low power load $P_0 = 10$ fW:

Type of bolometer	Energy of quantization	Characteristic parameter of absorber	NEP_{shot}
CEB	$k_B T_e = 9 \mu eV$	$T_e = 50 mK$	$1 * 10^{-19} W/Hz^{1/2}$
TES	$\Delta = 73 \mu eV$	$T_C = 500 mK$	$4 * 10^{-19} W/Hz^{1/2}$
KID [11,12]	$\Delta = 200 \mu eV$	$T_C = 1.2 K (Al)$	$7 * 10^{-19} W/Hz^{1/2}$

The lowest NEP can be achieved for CEB with lowest level of quantization. However, even these extreme parameters of P_0 and E_{quant} show that it's rather unrealistic to achieve $NEP=10^{-20}$ W/ Hz^{1/2} announced in NASA requirements for future missions [2].

Systems with linear on T thermal conductance

- Spider-web TES with conductance through the legs
 - CEB with cooling through SIN tunnel junctions (weak dependence on T: $G \sim T^{1/2}$),
- Limit shot noise is described by general formula (8) with numerical coefficient 2.

Systems with dominant e-ph thermal conductance (strong nonlinearity on T: $G_{e-ph} \sim T^4$):

- all bolometers on plane substrates with e-ph conductance
- antenna-coupled TES on chip with Andreev mirrors, - NHEB with Andreev mirrors.

Due to strong nonlinearity of e-ph conductance the limit shot noise is described by modified general formula with five times increased coefficient 10:

$$NEP_{shot-e-ph} = (10P_0 E_{quant})^{1/2} \tag{9}$$

That means if we leave the system for normal relaxation of energy through e-ph interaction, the shot noise is increased due to strong nonlinear dependence of electron-phonon thermal conductance on temperature in contrast to linear systems with weak dependence on temperature (or absence of it). These formulae (8,9) can be effectively used for estimation of ultimate parameters of CEB and other bolometers for given parameters of detector systems.

Quantum efficiency

Limit shot noise formula (9) gives estimation of the NEP in dependence of two parameters: background power P_0 and energy of quantization E_{quant} . Dependence on the P_0 is rather evident: the more incoming power is applied the higher noise of sensing element for any realization. Usually we could not change too much this parameter and realization is determined by external conditions. The second parameter, E_{quant} , is considerably more important for realization of limit NEP. This level of energy characterizes the quantum efficiency of bolometers (Fig. 5). Excitation of an electron for typical frequency of 1 THz to the level of 4 meV after consumption of the energy quantum is the same for all concepts. Then, relaxation of energy due to e-e interaction occurs to different energy levels.

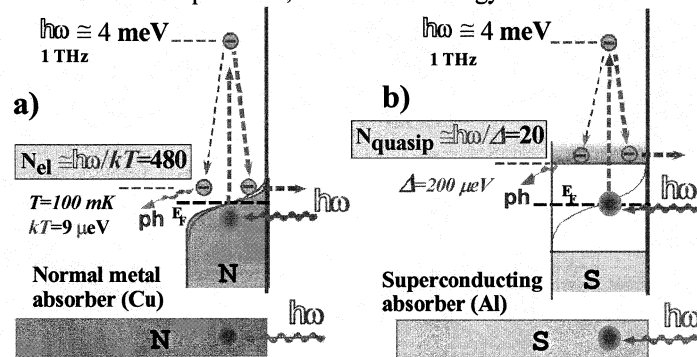
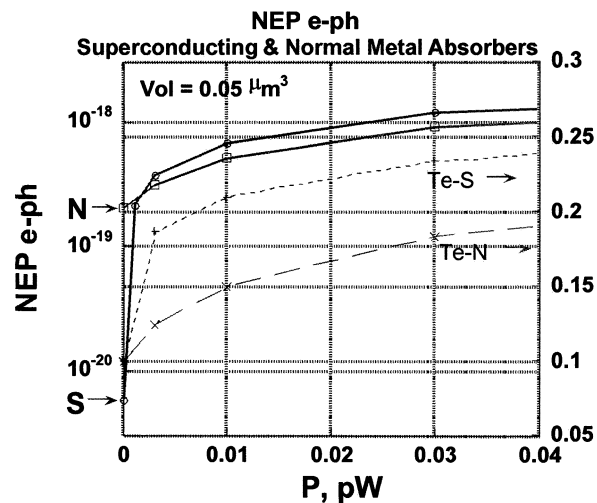


Fig. 5. Quantum efficiency of normal metal (a) and superconducting (b) absorber. An electron is excited after absorption of photon to the same energy level (4 meV for 1 THz signal) in both absorbers. Then electron is relaxed due to e-e interactions and energy is distributed between hot electrons at quantization level $E_{quant} = kT$ for normal metal (a) and between quasiparticle at quantization level $E_{quant} = \Delta$ for superconductor (b). The quantum efficiency is equal to 480 for normal metal and 20 for superconductor.

For CEB the energy will be distributed between electrons at the level of $kT=9 \mu eV$ (Fig. 5a). It gives number of electrons and quantum efficiency after absorption of one quantum: $N=480$ el/quant for electron temperature 100 mK. For TES and KID the relaxation of energy is stopped at the level of superconducting gap (Fig.5 b) that gives the following quantum efficiency: $N= 96$ for TES (with $\Delta=45 \mu eV$) and $N= 20$ for KID (with $\Delta=200 \mu eV$). Thus introduction of superconducting absorber considerably decreases the quantum efficiency that leads to higher shot noise and require more sensitive readout electronics.

Electron-phonon noise of superconducting and normal metal absorbers



Application of superconducting absorber for different bolometers is rather widespread due to opportunity of superconductor to absorb high frequency signals with energy quantum more than superconducting energy gap [10-14]. The theory of electron-phonon interaction in superconductors is complicated and an approximate scheme has been used for analysis of electron-phonon noise in

Fig. 6. Electron-phonon Noise Equivalent Power (NEP) for superconducting and normal metal absorbers in dependence on power load. Effective electron temperature is shown for illustration of overheating of the absorbers. Phonon temperature is equal to 100 mK. Dependence of electron temperature for uncooled CEB is shown for comparison.

superconductor [15] based on kinetic equation proposed in Ref. [16]. To illustrate complicated nature of superconducting absorber, the electron-phonon noise is compared for both superconducting and normal metal absorbers in dependence on power load (Fig. 6). The NEPe-ph has been estimated for phonon temperature $T=100$ mK and volume of the absorber equal to $0.05 \mu\text{m}^3$. Dependence of NEP for normal metal absorber does not show any unpredictable behavior: starting from $\text{NEP}=2 \cdot 10^{-19} \text{ W/Hz}^{1/2}$ it is monotonically increased for higher power. The superconducting absorber shows very low noise at zero power: $\text{NEP}=0.8 \cdot 10^{-20} \text{ W/Hz}^{1/2}$. It corresponds to some protection by superconducting gap against any excitations with energy less than Δ (Fig. 5b). However, even for very low applied power (> 1 fW), the noise is quickly increased to the level higher than NEP for normal metal. The reason of this noise is the same as discussed in previous paragraph. The quasiparticles excited by incoming signal are stopped at the level of Δ . Then recombination to superconducting state is accompanied by emitting of energetic phonons that lead to increased noise. Thus, protection of absorber by the gap without power load turns round in stopper of incoming energy at this higher level of the gap that leads to increased noise.

Optimal performance of the CEB

Our analysis of influence of the background power load on noise performance for different configurations of the CEB shows that the optimal configuration of the bolometer is the CEB with voltage-biased SIN tunnel junctions and current readout by a SQUID [8]. For analysis of ultimate performance, the high parameters of bolometer are accepted: a volume of absorber is equal to $0.01 \mu\text{m}^3$, which is realistic for modern technology, the current noise of SQUID is equal to $5 \text{ fA/Hz}^{1/2}$ [18]. The typical junction resistance (R) equal to $1 \text{ k}\Omega$ has been used for simulation. The results are shown in Fig. 9 for the level of microwave background power $P_0 = 0.01 \text{ pW}$. The latter figure is a relatively low level of background power load P_0 and used for analysis of limit characteristics of the CEB. The total $\text{NEP} = 1.2 \cdot 10^{-19} \text{ W}$ is determined mainly by shot noise of NIS tunnel junctions due to incoming power load. Electron-phonon component and amplifier noise are lower than noise of the NIS junction that corresponds to background limited case. Responsivity $S=dV/dP$ has maximum value of 150 nA/pW and is determined mainly by electron temperature of the absorber (energy of quantization) and finally by quantum efficiency of the CEB. For comparison, the similar figure, $S=200 \text{ nA/pW}$ can be achieved for TES for the case of relatively low bias voltage $V_b = 5 \mu\text{V}$.

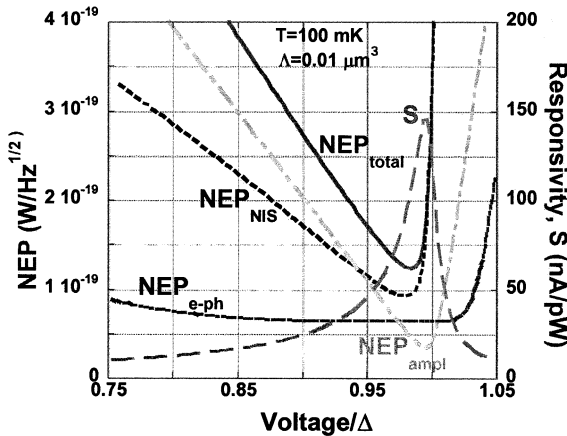


Fig. 7a. NEP of an optimal bolometer in presence of the background power load 0.01 pW for $\Delta = 0.01 \mu\text{m}^3$, $R = 1 \text{ k}\Omega$, $S_{\text{SQUID}} = 5 \text{ fA/Hz}^{1/2}$, and for bath temperature 100 mK .

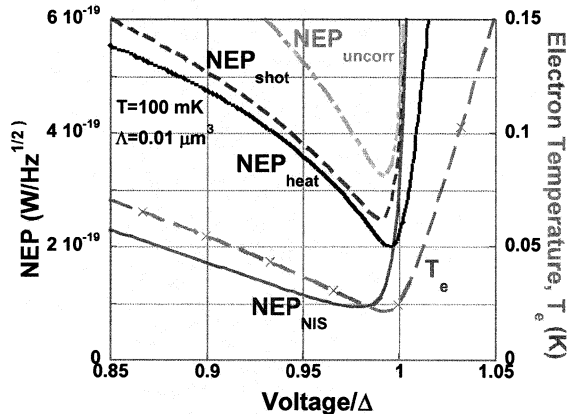


Fig. 7b. NEP_{SIN} with partial cancellation of the shot noise NEP_{shot} by the heat flow noise NEP_{heat} of SIN tunnel junction (7); $\text{NEP}_{\text{uncorr}}$ is shown for comparison.

It is interesting to analyze the correlated NEP_{SIN} (Fig. 7b) and uncorrelated $\text{NEP}_{\text{uncorr}}$ including the first and third terms in equation (7). The shot noise and heat flow noise (7), partly compensate each other due to mutual correlation and lead to reduction of NEP_{SIN} in comparison with NEP_{shot} . The reduction of noise is especially considerable when bias point deviates from delta more than kT_e and removed quantum of energy are more uniform that leads to closer values of shot and heat flow components and more effective compensation. This compensation is possible only in voltage-biased mode; in current-biased mode there would be opposite effect of increase of the noise higher than uncorrelated noise $\text{NEP}_{\text{uncorr}}$ [7-9].

We have analyzed the concept of the optimal CEB for 300 mK operation in the presence of the final background power load ($P_0 = 0.1 \text{ pW}$) and for fixed parameters of the SQUID-amplifier [8]. The optimal regime can be realized when thermal “cooling conductance” through the tunnel junctions predominates over “fundamental” electron-phonon conductance. In these circumstances, an NEP level of $10^{-18} \text{ W/Hz}^{1/2}$ at 300 mK can be achieved in presence of $P_0 = 0.1 \text{ pW}$ for typical parameters for junction resistor $R = 1 \text{ k}\Omega$, $S_{\text{SQUID}} = 10 \text{ fA/Hz}^{1/2}$, and a volume of the absorber $\approx 0.005 \text{ }\mu\text{m}^3$. This volume of the absorber is close to the technological limit.

Superconducting Cold-Electron Bolometer (SCEB) with Proximity Traps

Optimization of the CEB [8] has shown that the best values of NEP can be achieved for volumes less than $0.005 \text{ }\mu\text{m}^3$ representing the limit of technology that meet some problems in realization. Proposed concept of the SCEB with proximity traps (Fig. 8) helps to overcome these problems [18]. The best properties of the superconducting absorber without power load and normal metal absorber under power load (Fig. 6) are combined in this concept.

The bolometer consists of a superconducting antenna coupled by tunnel junctions to a narrow absorber with two proximity traps formed by square normal metal underneath the superconducting strip. The THz signal is concentrated by antenna and absorbed by superconducting strip having energy gap less than photon quantum (Fig. 8). The released heat diffuses to normal metal traps provided by the proximity effect in bilayer of superconductor-normal metal. The normal metal trap is simultaneously a top electrode for the SIN tunnel junction. Thermal isolation is provided by a potential barrier of the SIN tunnel junction (2eV) that should give perfect isolation up to optical range. SIN tunnel junctions remove the heat from the traps very effectively due to small volume of the normal metal. Tunnel junctions realize near 100% efficiency (!) as electron cooler (relation of area of the tunnel junction to the area of cooled absorber).

The NEP of the SCEB can be estimated using results of analysis of optimal bolometer in paragraph 3 [8]. Superconducting part of the absorber will not contribute to noise due to weak electron-phonon interaction for temperatures considerably lower than the gap. The typical volume of normal metal part of absorber is $\Lambda = 0.004 \text{ }\mu\text{m}^3$ ($0.5 \times 0.5 \times 0.02 \text{ }\mu\text{m}^3$) and is close to optimal value for best noise performance. The total NEP ([8]) for $P_0 = 0.1 \text{ pW}$, $R = 1 \text{ k}\Omega$, $S_{\text{SQUID}} = 10 \text{ fA/Hz}^{1/2}$, and $T = 300 \text{ mK}$ is at the level of $1.5 \times 10^{-18} \text{ W/Hz}^{1/2}$. In reality the effective volume of the traps can be even smaller due to proximity effect.

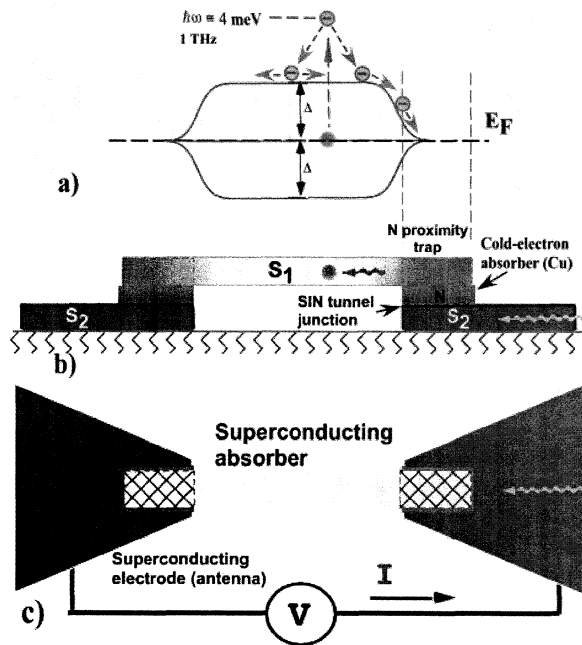


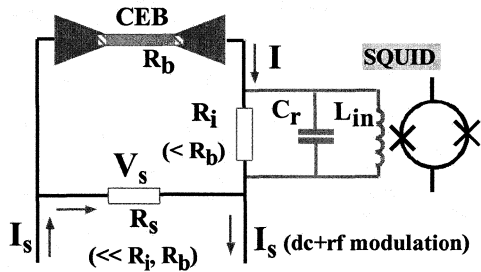
Fig. 8. Schematics of the cold-electron bolometer (SCEB) with superconducting absorber and proximity traps for very efficient electron cooling by the SIN tunnel junctions. a) The THz signal is concentrated by an antenna and absorbed by a superconducting strip having an energy gap less than the photon quantum. The released heat diffuses to normal metal traps provided by the proximity effect in bilayer of superconductor-normal metal. Side view b) and top view c) show layout of the bolometer. The SIN tunnel junctions remove a heat from the traps very effectively due to small volume of the normal metal forming top electrode of the tunnel junction and 100% area efficiency of cooling junctions.

Superconducting cold-electron nanobolometer (SCEB) with proximity traps and capacitive coupling to the antenna can be used in voltage-biased and current-biased modes. The voltage-biased mode could be optimized using more complicated parallel collection of tunnel junctions (twice increase of output current) [18].

Readout system.

The SQUID readout system with superconducting transformer and ferromagnetic core (Fig. 1) is under development [19]. Sensitivity of system is realized at the level of $30 \text{ fA/Hz}^{1/2}$. However, the main disadvantages of the system are large time constant, τ_{tr} , and excess noise of the ferromagnetic core. The large τ_{tr} closes a way to realization of full cooling ability of the CEB demanding time constant less than e-ph time constant. The large τ_{tr} close a way to

realization of multiplexing schemes with large number of channels. The SQUID with resonance circuit (instead of transformer) could help to overcome these difficulties and realize all advantages of CEB with very short time constant. Voltage-biased mode of CEB operation with modulation of bias voltage could be used in this case. This mode could be realized by using small voltage bias resistor $R_s \ll R_i, R_b$. The voltage V_s is



applied to the CEB and the task is to measure RF component of current I through the CEB with maximum sensitivity. The optimal realization is parallel resonance circuit (with resonance

Fig. 9. SQUID readout system with RF modulation of the bolometer bias and resonance selection of the signal by input inductance of the SQUID and additional parallel capacitance. Quality factor of 100 can be easily realized for typical parameters of the SQUID (using input inductance), additional capacitance $C_r = 3$ nF and current measuring resistor $R_i = 1$ k Ω .

of currents) connected in parallel to current measuring resistor R_i . The optimal value of $R_i = 1$ k Ω for typical bolometer dynamic resistance from 1 to 10 k Ω . For quality factor $Q = 100$, current SQUID sensitivity could be improved from 1 pA/Hz^{1/2} to 10 fA/Hz^{1/2} that is a goal of current measurements. For modulation frequency 5 MHz and input SQUID inductance $L_{in} = 0.3$ μ H, we would get inductive impedance $Z_L = \omega L = 10$ Ω and $C_r = 3$ nF. This impedance gives a searched quality factor $Q = R_i/Z_L = 100$. This schematic gives opportunity to get high sensitivity of readout system and select channels for frequency domain multiplexing.

Conclusions

The concept of a cold-electron bolometer with strong electrothermal feedback is a turning point in development of supersensitive detectors from artificial bias heating to effective electron cooling. This concept could give the ultimate noise performance in presence of a realistic background power load. Due to strong electrothermal feedback, all incoming power is removed with high accuracy from the absorber increasing dynamic range of the system. The CEB does not suffer from the problem of saturation showing only some deviation from the linear response for power higher than characteristic cooling power. The time constant of CEB could be considerably reduced by the loop gain of negative electrothermal feedback (similar to TES) to the level of 10 ns. The CEB concept could be very promising for future post-Herschel space telescopes.

The author would like to thank Paul Richards, Dmitri Golubev, and Michael Tarasov for stimulating discussions. The work was supported by VR and SI Swedish agencies.

1. BREAKTHROUGH OF THE YEAR 2003: "Illuminating the Dark Universe". Science, **302**, p.2038 (2003).
2. D. Leisawitz et al., "Scientific motivation and technology requirements for the SPIRIT and SPECS far-infrared/submillimeter space interferometers", SPIE 2000.
3. K. Irwin. Applied Physics Letters, **66**, (1995) 1998.
4. A. Lee, P. Richards, S. Nam, B. Cabrera, K. Irwin, Applied Physics Letters, **69**, (1996) 1801.
5. L. Kuzmin, Proceeding of the 9th International Symposium on Space Terahertz Technology, Pasadena, pp 99-103, March 1998; Physica B: Condensed Matter, **284-288**, (2000) 2129.
6. L. Kuzmin, I. Devyatov, and D. Golubev. Proceeding of SPIE, v. 3465, pp. 193-199 (1998).
7. D. Golubev and L. Kuzmin. Journal of Applied Physics. **89**, 6464-6472 (2001).
8. L. Kuzmin and D. Golubev. Physica C **372-376**, pp 378-382 (2002).
9. S. Golwala, J. Johm, and B. Sadoulet, Proceedings of the VIIth International Workshop on Low Temperature Detectors, July 1997, Munich, Germany, pp 64-65.
10. B. Mazin, P. Day, J. Zmuidzinas, and H. LeDuc, AIP Conference Proceedings **605**, pp. 309-312, July 2001.
11. A. Sergeev, V. Mitin, and B. Karasik, Appl. Phys. Lett. **80**, 817-819 (2002).
12. A. Peacock et al., Nature **381**, (1996) 135.
13. R.J. Schoelkopf et al., IEEE Transactions on Applied Superconductivity, **9** (1999) 2935.
14. A.D. Semenov, G.N. Gol'tsman, and A.A. Korneev, Physica C, **351** (2001) 349.
15. D. Golubev and L. Kuzmin, "Superconducting hot-electron bolometer", to be published.
16. J. Clarke, in Nonequilibrium superconductivity, ed. by D. Langenberg and A. Larkin, Elsevier S.Publ (1986).
17. F. Gay, F. Piquemal, G. Geneves, Rev. Sci. Instr., V. 71, N 12, 4592-4595 (2000).
18. L. Kuzmin, Microelectronic Engineering, **69**, 309-316 (2003).
19. M. Tarasov, S. Gudoshnikov, A. Kalabukhov, H. Seppa, M. Kiviranta, L. Kuzmin, Physica C 368, 2002, p. 161-165.